



APPENDIX F
HEAT TRANSFER MODEL DERIVATION
METHANE EXPLOSION

APPENDIX F

HEAT TRANSFER MODEL DERIVATION

METHANE EXPLOSION

Under the conditions of a postulated methane explosion within the panel, the temperature of the gas is raised by the combustion process to an initial value $T_{g \text{ init}}$ with time $t = 0$ corresponding to initial conditions in the panel. Subsequently, the gas temperature in the panel decreases as heat is transferred to the surrounding salt and to the two explosion-isolation walls in the air-intake and air-exhaust drifts of each panel.

At time $t = 0$ the pressure in the panel is P_{init} based on panel closure due to creep and the elevation in pressure resulting from the explosion. Thus, the rise time of the temperature is not considered in the model.

At time $t = 0$, the volume of the panel is V_{init} and is assumed to remain constant throughout the cooling of the gas in the panel because of the short duration of the explosion. This means that the effect of creep on the panel volume is assumed negligible during the postulated explosion. The initial volume is given by:

$$V_{\text{init}} = V_{\text{panel}} - V_{\text{waste}} - V_{\text{creep}}$$

where

- V_{init} = Initial volume
- V_{panel} = Volume of the panel
- V_{waste} = Volume of the waste
- V_{creep} = Volume reduction due to creep



and is taken as given at the start of the heat transfer analysis and assumed to remain constant during the transfer of heat to the panel walls, roof, and floor.

F.1.0 Heat Balance

Assuming a constant volume is equivalent to stating that any creep closure of the panel volume during the explosion and subsequent cooling can be neglected.

$$\frac{dQ_{\text{volume of gas}}}{dt} = qA_{\text{walls, floor, roof}}$$

where $Q_{\text{volume of gas}}$ represents the heat contained in the hot gases subsequent to an explosion, q is the heat flux rate at the boundaries of the panel volume, and $A_{\text{walls, floor, roof}}$ is the surface area of the panel volume.

Following D'Appolonia (1978) it is conservatively assumed that the heat transfer to the surrounding walls, floor, roof, is related to the rate of change of enthalpy of the reaction products gas. Thus, the heat content of the room is given by:

$$\frac{dQ_{\text{volume of gas}}}{dt} = nC_p \frac{dT_g}{dt}$$

where n is the number of moles of gas in the room subsequent to the explosion, T_g is the gas temperature, and C_p is the heat content of the gas at constant pressure.¹ Thus,

$$nC_p \frac{dT_g}{dt} = qA_{\text{walls, floor, roof}} \quad (1)$$

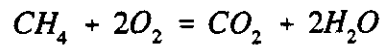
F.2.0 Moles of Gas

The gas in the panel subsequent to the explosion is a mixture of the combustion products of the explosive gas which is taken to be a mixture of methane, CH_4 and air. Because methane can explode with other than a stoichiometric air/methane mixture (i.e., the methane concentration in air for an explosion to occur is a range as opposed to a single value), it is impossible to determine the number of moles of combustion product gas precisely. Thus, it is assumed that the explosion occurs with a stoichiometric air/methane mixture.

¹The specific heat at constant volume is used even though the explosion or rapid combustion of the methane-air mixture occurs at constant volume because the rate of change of enthalpy as opposed to internal energy has been used.

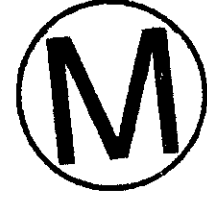
F.2.1 Mixture

The stoichiometric reaction for methane is (Bodantha, 1980):



with the moles of air given by:

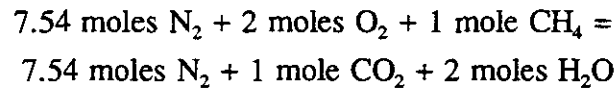
$$n_{\text{air}} = 4.77(2) = 9.54 \text{ mole air/mole methane}$$



or 9.54 moles of air are required to provide 2 moles of oxygen. Using a ratio of 9.54 moles of air per mole of methane, the total moles of gas at the time of the explosion would be:

$$n = (9.54 + 1)n_{\text{CH}_4}$$

The number of moles of nitrogen in the air and in the combustion products gas is $3.77(2) = 7.54$ moles/mole of methane (Bodantha, 1980). Thus,



On a molar basis the reaction products are 71.5% nitrogen, 9.5% carbon dioxide, and 19% water vapor. This compares with a reaction product that is 72.9% nitrogen, 11.6% carbon dioxide and 15.5% water vapor when propane is burned at a stoichiometric ratio (D'Appolonia, 1978). Also, 10.54 moles of the methane-air mixture produces 10.54 moles of reaction products. Thus, the number of moles of air/methane prior to the explosion is the same as the number of moles of the product gas and the above relation for n will be used to compute the heat content in a panel prior to cooling.

$$n_{\text{gas}} = 10.54 n_{\text{CH}_4} \quad (2)$$

Substituting (2) into (1),

$$10.54 n_{\text{CH}_4} C_p \frac{dT_g}{dt} = qA_{\text{walls, floor, roof}}$$

or

$$\frac{dT_g}{dt} = \frac{qA_{\text{walls, floor, roof}}}{10.54 n_{\text{CH}_4} C_p} \quad (3)$$



is the differential equation for the time rate of change of the gas temperature in the panel following an explosion.

F.2.2 Specific Heat

The specific heat, C_p , of the combustion products of the explosion is required by equation (3). In general, the specific heat is a function of temperature over large temperature ranges. Figure C-1 shows plots of specific heats of the combustion products of stoichiometric propane-air mixtures and methane-air mixtures based on data from D'Appolonia (1978) and Reid, et al., (1977). The curves for propane-air mixtures are shown for comparison between the Reid, et al. data and the D'Appolonia data.

For an explosion temperature on the order of 2400 degrees kelvin ($^{\circ}\text{K}$), and using an average of the wall temperature and gas temperature to evaluate the specific heat, the temperature dependence curve will be evaluated in the region of 1400 $^{\circ}\text{K}$ which is about the maximum useful temperature for the Reid, et al. data.

As shown on Figure F-1, the Reid et al. (1977) and D'Appolonia (1978) data agree well up to a temperature of approximately 1400 $^{\circ}\text{K}$. At the greater temperatures Reid et al. (1977), and other data indicate a decrease in specific heat with greater temperatures which is not consistent with expectation.

Figure F-2 shows a comparison of Reid et al. (1977) and the D'Appolonia (1978) data multiplied by 0.961, the ratio of specific heats for a methane-air mixture to a propane-air mixture at 300 $^{\circ}\text{K}$. Below 1400 $^{\circ}\text{K}$ the agreement is very good. Above 1400 $^{\circ}\text{K}$ the curve based on the D'Appolonia data remains valid. Therefore, the specific heat of the combustion products formed from a stoichiometric methane air mixture as a function of temperature is²

$$C_p = 1.29 \times 10^{-3} T + 7.3353 - \frac{32682}{T^2} \quad (4)$$

²Equation (4) was obtained by multiplying Equation (9) of Appendix B of D'Appolonia [1978] by 0.961.

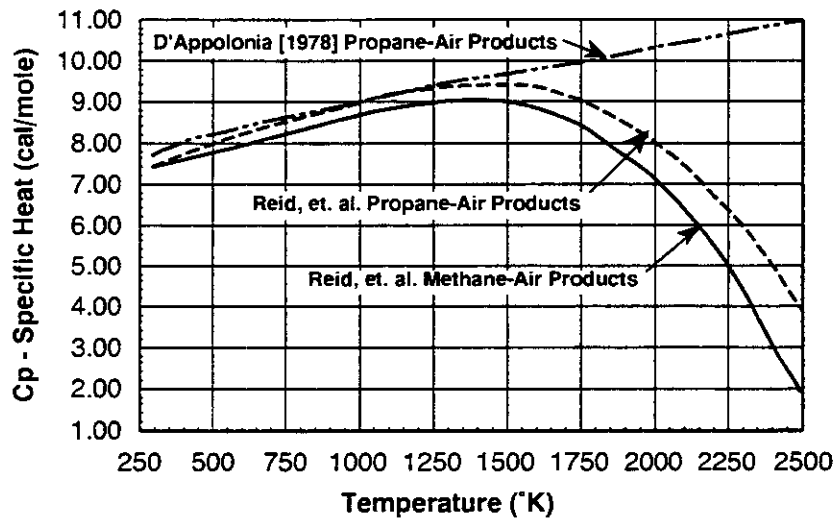


Figure F-1
Specific Heat as a Function of Temperature

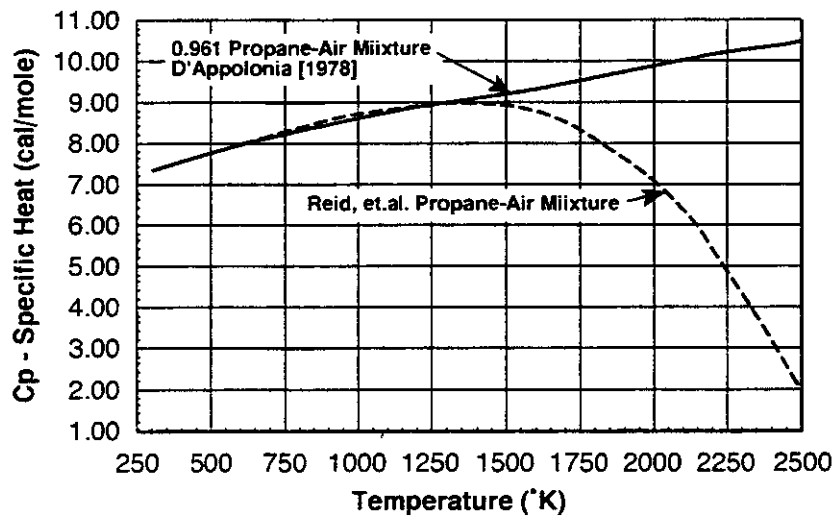


Figure F-2
Specific Heat for Methane-Air Stoichiometric Mixture

F.3.0 Heat Transfer to the Walls, Floor, Etc.

Heat is transferred from the gas to the surrounding walls, floor and roof of the panel rooms by both convection and radiation. Heat is then transferred into the walls, floor, roof, via conduction. Thus, the rate of heat conduction into the salt or the wall is governed by the rate at which heat can be conducted into the solids.

F.3.1 Radiation Heat Transfer

Heat transferred from the gas to the walls, floor, roof, is given by:

$$q_{rs} = \sigma(T_g^4 - T_w^4)$$

where q_{rs} is the heat flux to the walls, floor, roof, σ is the Stefan-Boltzmann constant (1.35×10^{-12} cal/cm²-sec-°K), and T_w is the temperature of the walls, floor, and roof.

The majority of the surface area of the panel available for heat transfer via both radiation and convection is salt. However, a small portion of the total area will be the inner face of the explosion-isolation wall (or construction-isolation well). Because the wall, floor, roof temperature is controlled by the time dependent conduction of heat into either the walls, floor, roof or the wall faces, and the diffusivities and conductivities of the salt and wall, floor, roof material may be different, the radiation heat transfer is divided into two components.

The radiative heat transfer to the salt (T_{ws}) is:

$$q_{rs} = \sigma(T_g^4 - T_{ws}^4)$$

and the radiative heat transfer to the explosion-isolation wall (T_{wb}) is:

$$q_{rb} = \sigma(T_g^4 - T_{wb}^4)$$

The combined radiative heat transfer to the walls, floors, roof is:

$$Q_r = q_{rs}A_s + q_{rb}A_b$$

or

$$Q_r = \sigma \left(A_s [T_g^4 - T_{ws}^4] + A_b [T_g^4 - T_{wb}^4] \right) \quad (5)$$

where A_b = Area of the walls, and A_s = area of the salt.

Equation (5) comprises the radiation portion of the right hand side of the differential equation, (3), for the rate of gas temperature in the panel.

F.3.2 Convection Heat Transfer

In addition to radiation, heat is transferred to the walls, floor, roof, and explosion-isolation walls by natural convection. In subsequent discussion, walls denote all exposed surface area of salt within a panel. Explosion-isolation walls denote the surface area of the expendable walls placed in the sealed air-intake and air-exhaust drifts of the panel.

F.3.2.1 Heat Transfer from Gas to the Walls

In addition to radiation, heat is transferred to the walls, floor, roof, and explosion-isolation walls via natural convection. The heat flux due to convection (q_c) is given by:

$$q_c = h(T_b - T_w)$$

where h = Film coefficient.

As for the case of radiation, the majority of heat transfer by convection will occur to the surrounding salt. However, a portion will be transferred to the explosion-isolation wall. Because the temperature of the explosion-isolation wall may be different from the temperature of the salt, the convective heat transfer is divided into the two components analogous to the radiation heat transfer. For the salt, the convection heat transfer is:

$$q_{cs} = h(T_g - T_{ws})$$

and for the explosion-isolation walls:

$$q_{cb} = h(T_g - T_{wb})$$

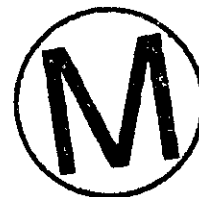
The combined radiative heat transfer (Q_c) to the walls, floors, roof, and explosion-isolation walls is:

$$q_{cb} = h(T_g - T_{wb})$$

The combined radiative heat transfer (Q_c) to the walls, floors, roof, and explosion-isolation walls is:

assuming that the heat transfer coefficient does not change with location or material.

$$Q_c = q_c NaCl A_s + q_{cb} A_b$$



Theoretically the convective heat transfer coefficient is different for the face of the explosion-isolation walls, which are vertical compared with the heat transfer coefficient for the roof and floor faces of the panel which are horizontal. Neglecting the difference in heat transfer coefficient due to geometric differences, the above two equations for the heat flow to the walls, floor, roof, and explosion-isolation walls can be combined to give

$$Q_c = h \left(A_s [T_g - T_{ws}] + A_b [T_g - T_{wb}] \right) \quad (6)$$

Equation (6) gives the convective heat transfer portion of the right hand side of Equation (3). Combining (3), (5) and (6),

$$\frac{dT_g}{dt} = - \frac{Q_c + Q_r}{10.54 n_{CH4} C_p} \quad (7)$$

where the negative sign indicates that Q_c and Q_r represent heat transferred out of the system consisting of the gas in the room. These same quantities then represent heat transferred into the surrounding salt and explosion-isolation wall.

F.3.2.2 Convection Coefficient

Assuming the convection coefficient is the same at all surfaces and following the methods developed in D'Appolonia (1978), with all units in the centimeter-gram-second (cm-g-sec) system of units,

$$N_u = 0.13[P_r G_r]^{1/3}$$

where P_r is the Prandtl number and G_r is the Grashof number. The Prandtl number is essentially constant and is taken as 0.71 regardless of pressure and temperature. The Grashof number is given by

$$G_r = \frac{g\beta L^3(T_g - T_w)}{\nu^2}$$

where g is the acceleration of gravity, β is the volume coefficient of thermal expansion and ν is the kinematic viscosity of the gas. For ideal gases,

$$\beta = \frac{1}{T_g}$$

and the kinematic viscosity is given by

$$\nu = \frac{\mu}{\rho}$$

where μ is the absolute viscosity ρ = mass density. Substituting for ν and β in the expression for the Grashof number,

$$G_r = \frac{g\rho^2 L^3(T_g - T_w)}{T_m \mu^2}$$

where

$$T_m = \frac{T_g + T_w}{2}$$



is the average of the gas and surface temperature.

Substituting for the Grashof number and Prandtl number in the expression for the Nusselt number,

$$N_u = 0.13 \left(0.71 \frac{g \rho^2 L^3 [T_g - T_w]}{T_m \mu^2} \right)^{1/3}$$

$$N_u = 0.146 L \left(\frac{g \rho^2 \left[\frac{T_g - T_w}{T_g + T_w} \right]}{\mu^2} \right)^{1/3}$$

and substituting for the Nusselt number in the expression for the convection coefficient,

$$h = 0.146 k_g \left(\frac{g \rho^2 \left[\frac{T_g - T_w}{T_g + T_w} \right]}{\mu^2} \right)^{1/3}$$

Since the thermal conductivity of the gas is given by³

$$k_g = 6.4 \times 10^{-5} \left(\frac{T_m}{300} \right)^{.75}$$

$$h = 9.34 \times 10^{-6} \left(\frac{T_g + T_w}{600} \right)^{.75} \left(\frac{g \rho^2 \left[\frac{T_g - T_w}{T_g + T_w} \right]}{\mu^2} \right)^{1/3} \quad (8)$$

Figure F-3 shows h as a function of surface temperature based on a gas temperature of 2400°K and density and viscosity consistent with conditions at the time of an explosion.

Assuming that no additional gas is generated subsequent to the explosion, the density of the gas after the explosion is the same as before the explosion since mass is conserved. Thus, the gas density after the explosion is the molecular weight of n moles of methane plus 9.54n moles of air divided by the initial volume,

³D'Appolonia [1978].

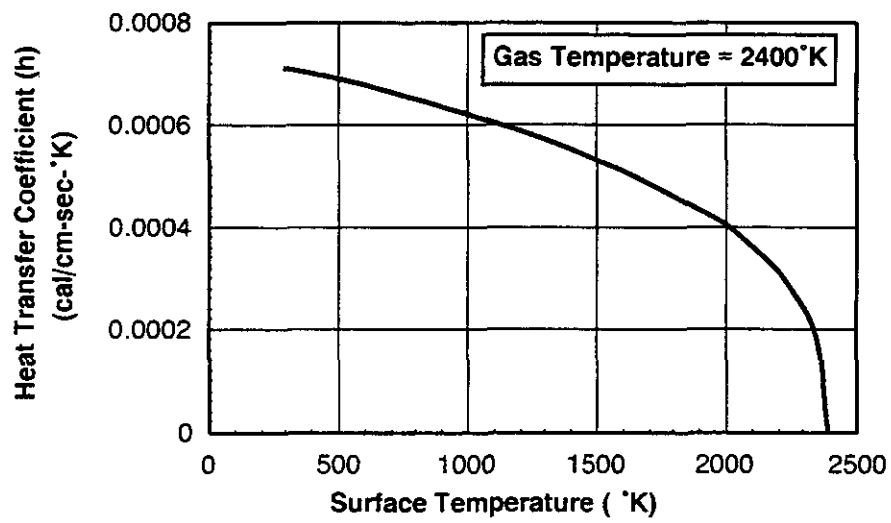


Figure F-3
Convection Heat Transfer Coefficient Versus Temperature

$$\rho = n \left(\frac{M_w CH_4 + 9.54 M_w air}{V_{init}} \right)$$

$$\rho = n \left(\frac{16 + 9.54(29)}{V_{init}} \right)$$

$$\rho = \frac{292.66n}{V_{init}} \quad (9)$$

$$\mu = 1.85 \times 10^{-4} \left(\frac{T_m}{300} \right)^{0.67} \quad (10)$$



and the viscosity is given by (D'Appolonia, 1978), where the viscosity is evaluated at the average of the surface and gas temperatures.

Because there will be two different surface temperatures, one corresponding to the salt, and one for the explosion-isolation wall, there will be different convective heat transfer coefficients as well.

F.3.3 Conduction Into the Walls, Floor, Roof, and Explosion-Isolation Walls

The temperature which controls the heat transfer from the gas via radiation and convection is controlled by the rate at which heat is conducted into the walls, roof, floor, and explosion-isolation walls. The diffusion of heat into the walls, floor, roof, and explosion-isolation walls is assumed to be governed by a one-dimensional, semi-infinite thermal diffusion model. If the temperature penetrates the explosion-isolation walls, the model is changed to be thermal diffusion across a slab of finite thickness with an ambient gas temperature on the side in the isolation zone.

Thermal diffusion into the walls, floor, roof, and explosion-isolation walls is governed by the partial differential equation,

$$\alpha \frac{\partial^2 T}{\partial x^2} = \frac{\partial T}{\partial t}$$

where α is the thermal diffusivity, T is the temperature, x is the distance into the wall, floors, roof, or explosion-isolation walls, and t is time. At $x = 0$ the flow of heat into the walls, floor, roof, or explosion-isolation walls is governed by the boundary condition,

$$-k \frac{\partial T}{\partial x} = q_{in}$$

where q_{in} is the heat flux into the walls, etc. from the gas via convection and radiation and k is the thermal conductivity. Because the thermal diffusivity and conductivity for salt is different from that of the explosion-isolation wall, two conduction models are required.

F.3.3.1 Heat Conduction to the Salt

The first involves the heat transferred from the gas to the salt and is governed by the partial differential equation,

$$\alpha_s \frac{\partial^2 T_s}{\partial x^2} = \frac{\partial T_s}{\partial t} \quad (11i)$$

where α_s is the thermal diffusivity of salt which is a function of temperature. Figure F-3 shows plots of thermal diffusivity for halite, anhydrite, argillaceous halite and polyhalite (Krieg, 1983). Figure F-4 also shows data from D'Appolonia (1978) that used the relation

$$\alpha_s = \frac{10}{T_s}$$

for salt. The D'Appolonia temperature dependence yields slightly higher values compared with the Waste Isolation Pilot Plant (WIPP) data, but indicates a consistency in the data. For purposes of the post-explosion heat transfer analysis the temperature dependent data for salt has been used.

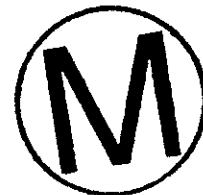
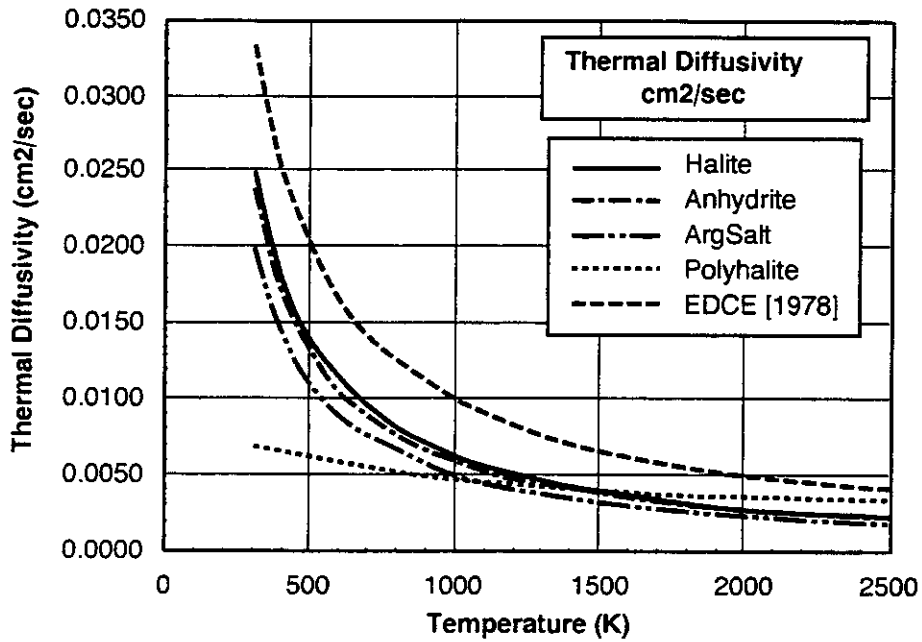


Figure F-4
 Thermal Diffusivity of WIPP Geologic Materials

$$\alpha_s = 0.025 \left[\frac{300}{T_s} \right]^{1.14} \quad (12i)$$

The boundary condition at the surface of the salt is:

$$-k_s \frac{\partial T_s}{\partial x} = q_{sr} + q_{sc} \quad (13i)$$

where k_s is the thermal conductivity of the salt. Figure F-4 shows plots of thermal conductivities for the same materials as a function of temperature. Again, the thermal conductivity from D'Appolonia (1978):

$$k_s = \frac{4.5}{T_s}$$

is also shown on Figure F-5 to check the consistency of the WIPP data. Again, the thermal conductivity for halite was used for the post-explosion heat transfer analysis.

$$k_s = 0.012 \left[\frac{300}{T_s} \right]^{1.14} \quad (14i)$$



The terms q_{sr} and q_{sc} in (13i) couple the heat conduction into the salt with the rate of cooling of the gas via equations (7) through (10). In addition to the boundary conditions given by (12i), initial conditions at time $t = 0$ are required. It is assumed that at $t = 0$ the salt is at the ambient temperature in the panel, T_{amb} . Equations (11i) through (14i) with the initial conditions form the complete problem for the temperature in the salt as a function of time as the gas cools following the explosion.

F.3.3.2 Heat Conduction to the Explosion-Isolation Walls

The second model involves the heat transferred from the gas to the explosion-isolation walls and is governed by the partial differential equation,

$$\alpha_b \frac{\partial^2 T_b}{\partial x^2} = \frac{\partial T_b}{\partial t} \quad (11ii)$$

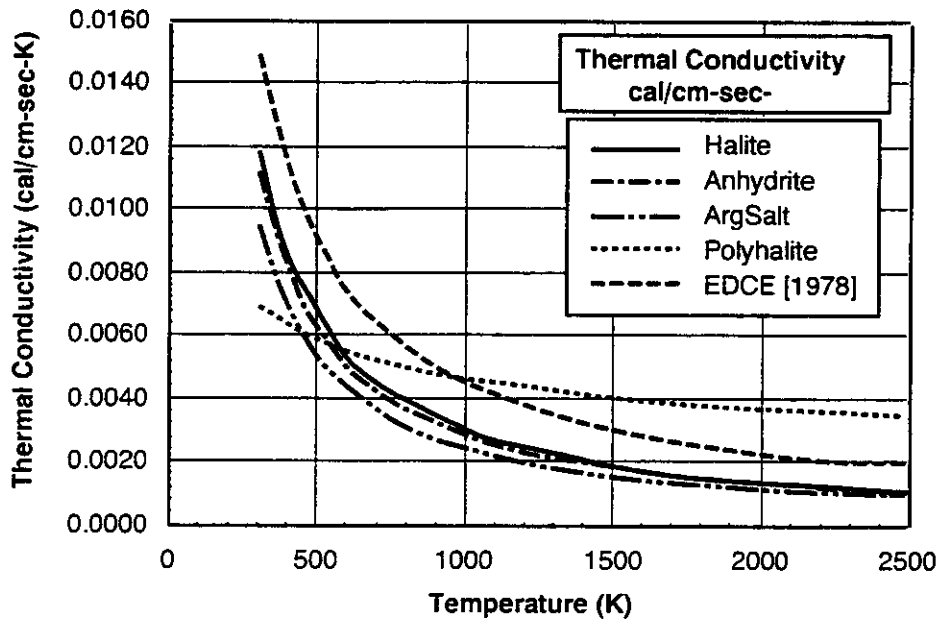


Figure F-5
Thermal Conductivity of WIPP Geologic Materials

where α_b is the thermal diffusivity of explosion-isolation walls. If the explosion-isolation walls are concrete, the thermal diffusivity does not vary with temperature (D'Appolonia, 1978),

$$\alpha_s = 0.005 \quad (12ii)$$

The boundary condition is:

$$-k_b \frac{\partial T_b}{\partial x} = q_{br} + q_{bc} \quad (13ii)$$

where q_{br} = heat flux for the salt, q_{bc} = heat flux for explosion-isolation walls, and k_b is the thermal conductivity of the walls. Again, if the explosion-isolation walls are concrete, the thermal conductivity is constant (D'appolonia, 1978).

$$k_b = 0.002 \quad (14ii)$$

Analogous to the case for salt, the terms q_{br} and q_{bc} in (13ii) couple the heat conduction into the salt with the rate of cooling of the gas via equations (7) through (10). At $t = 0$ the explosion-isolation walls are at the ambient temperature at the panel level, T_{amb} .

F.4.0 Numerical Model

Equations (1) through (14) were solved using a computer program based on an explicit finite difference representation of the equations. In subsequent discussion the following symbols are used,

- τ = time step Δt
- ϵ = distance between mesh points, Δx , in finite difference representation of semi-infinite solid used to model the explosion-isolation walls.
- n = subscript denoting the value of a variable at time t .
- $n+1$ = subscript denoting the value of a variable at time $t+\tau$.
- m = subscript denoting the value of a variable at mesh point m in a finite difference representation of a semi-infinite solid. $m = 0$ corresponds to the boundary $x = 0$.
- T_{gn} = gas temperature at time t .
- T_{s0} = temperature at $x = 0$ in salt.
- T_{b0} = temperature at $x = 0$ in an explosion-isolation wall.
- T_{smn} = temperature in salt at mesh point m and time n .
- T_{bmn} = temperature in explosion-isolation walls at mesh point m and time n .
- α_{sm} = thermal diffusivity in salt at mesh point m (function of temperature).

- α_{bm} = thermal diffusivity of explosion-isolation wall material at mesh point m (may be constant or a function of temperature).
- q_{rsn} = heat flux to wall (salt) via radiation at time point n.
- q_{rtn} = heat flux to explosion-isolation wall via radiation at time point n.
- q_{csn} = heat flux to wall (salt) via convection at time point n.
- q_{cbn} = heat flux to explosion-isolation wall via convection at time point n.

Where symbols are used for parameters that are a function of temperature and consequently also a function of time, the subscripts n and n+1 refer to whether the parameter is evaluated at t or t + Δt .

F.4.1 Overview of Computer Program

Figure F-6 provides a simplified flow chart of the computer program used to solve the equations in the model in explicit finite difference form.

F.4.2 Finite Difference Formulation

For the first pass through the calculational loop n = 0 and the gas temperature is set to T_{g0} , the initial temperature. Based on the assumption of constant volume during the explosion, the temperature is related to the pressure by,

$$T_{g0} = T_{gamb} \left(\frac{P_0}{P_{amb}} \right) = 8T_{gamb} \quad (15)$$

where

- T_{gamb} = the gas temperature prior to the explosion
- P_{amb} = the gas pressure prior to the explosion (taken as 2 atm)
- P_0 = the gas pressure caused by the explosion (taken as 16 atm)
- T_{g0} = the gas temperature caused by the explosion which is the initial gas temperature for the cooling analysis.

The initial temperature of the salt (T_{smo}) and explosion-isolation walls (T_{bmo}) for the heat conduction calculations are set to the ambient temperature at all mesh points.

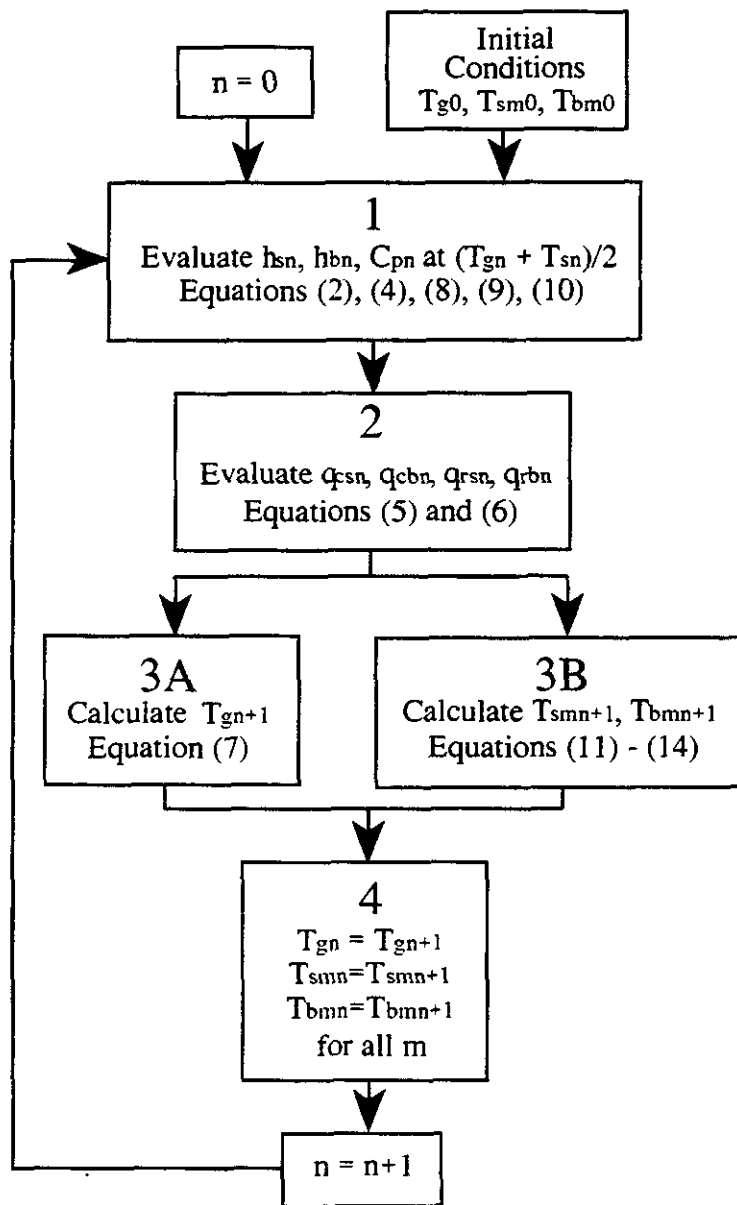


Figure F-6
Program Flow Chart


$$\begin{aligned} T_{sm0} &= T_{amb} \quad m = 1 \dots M \\ T_{bm0} &= T_{amb} \quad m = 1 \dots M \end{aligned} \tag{16}$$

where M is the maximum mesh point number used in the finite difference representation of the semi-infinite solid. T_{amb} is the ambient temperature of the salt and explosion-isolation wall at the time of the explosion.

F.4.2.1 Program Section 1

Section 1 of the program (Figure F-3) calculated the parameters required for the determination of the heat fluxes from the hot gas to the cooler walls. These calculations are performed initially based on values for $n = 0$, initial conditions. Subsequently, they are evaluated based on the temperature values at time point n .

Thus,

$$\begin{aligned} \mu_{sn} &= 1.85 \times 10^{-4} \left(\frac{T_{gn} + T_{s0n}}{600} \right)^{0.67} \\ \mu_{bn} &= 1.85 \times 10^{-4} \left(\frac{T_{gn} + T_{b0n}}{600} \right)^{0.67} \end{aligned} \tag{17}$$


where

μ_{sn} = viscosity of the salt

μ_{bn} = viscosity of the explosion-isolation wall

T_{gn} = gas temperature at time point n


T_{s0n} = wall temperature of the salt at time point n , which is the $m = 0$ mesh point of the finite difference representation of the semi-infinite solid used to model heat conduction into the salt

T_{b0n} = surface temperature of the explosion-isolation wall.

Since the initial surface temperatures of the salt and the walls are the same, the initial value of μ will be the same at both the salt and the walls. However, with time as the surface temperature of the explosion-isolation walls varies from the surface temperature of the salt, the values of μ will be different for the salt compared with the walls. This plays a role in

having different convection heat transfer coefficients at the salt compared with the explosion-isolation walls.

The convection heat transfer coefficients are given by (8) below.

$$\begin{aligned}
 h_{sn} &= 9.34 \times 10^{-6} \left(\frac{T_{gn} + T_{s0n}}{600} \right)^{75} \left(\frac{g\rho^2}{\mu_{sn}^2} \frac{T_{gn} - T_{s0n}}{T_{gn} + T_{s0n}} \right)^{1/3} \\
 h_{bn} &= 9.34 \times 10^{-6} \left(\frac{T_{gn} + T_{b0n}}{600} \right)^{75} \left(\frac{g\rho^2}{\mu_{bn}^2} \frac{T_{gn} - T_{b0n}}{T_{gn} + T_{b0n}} \right)^{1/3}
 \end{aligned}
 \tag{18}$$


The density, ρ , remains constant by virtue of the constant volume and constant number of moles. The acceleration of gravity, g , also remains constant for all time points.

The specific heat of the gas which is required for Section 3A of the program is given by (4) below.

$$C_{pn} = 6.45 \times 10^{-4} (T_{gn} + T_{s0n}) + 7.3353 - \frac{130728}{(T_{gn} + T_{s0n})^2}
 \tag{19}$$

Because the specific heat is a bulk property of all of the gas in the panel, it is affected by all of the surface area in the panel. Because the surface area of the salt is orders of magnitude larger than the surface area of the explosion-isolation walls, the specific heat at each time is based solely on the surface temperature of the salt.

F.4.2.2 Program Section 2

The heat flux rates to the walls as well as the total heat transfer rates to the walls via convection and radiation are calculated in Section 2 of the program. Flux is required for the boundary condition for the heat conduction analysis of Section 3B and total heat flow is required for the change in gas temperature calculation in Section 3A.

The total heat flow values are given by (5) and (6) which for time step n become where h_{sn} and h_{bn} are given by (18). The total heat flows are used in Section 3A of the program evaluates the time rate of change of the gas temperature using equation (7).

$$Q_{rn} + \sigma \left(A_s [T_{gn}^4 - T_{s0n}^4] + A_b [T_{bn}^4 - T_{b0n}^4] \right) \quad (20)$$

$$Q_{cn} = A_s h_{sn} (T_{gn} - T_{s0n}) + A_b h_{bn} (T_{gn} - T_{bn})$$

The total heat flows at time step n given by (20) are heat flow out of the gas occupying the panel volume and into the explosion-isolation walls. For the heat flow into the explosion-isolation walls, the areas, A_s and A_b cancel from the equations representing the boundary conditions at $x = 0$ for the transient heat conduction problems solved in Section 3B of the program. Thus, for Section 3B, the heat flux values are required. These are the same as (20) without the areas.

$$q_{rn} = \sigma \left([T_{gn}^4 - T_{s0n}^4] + [T_{bn}^4 - T_{b0n}^4] \right) \quad (21)$$

$$q_{cn} = h_{sn} (T_{gn} - T_{s0n}) + h_{bn} (T_{bn} - T_{bn})$$

where q_{rn} and q_{cn} are the heat fluxes due to radiation and convection.

For the total heat flow and heat flux due to radiation, the Stefan-Boltzmann constant is taken to be constant for all values of temperature and hence time.

$$\sigma = 1.355 \times 10^{-12} \quad (22)$$

F.4.2.3 Program Section 3

Section 3 comprises the main body of the program.

F.4.2.3.1 Program Section 3A

Equation (7) governs the rate of change of gas temperature in the panel volume. Using the explicit finite difference approximation,

$$\frac{dT_g}{dt} = \frac{1}{\tau} (T_{gn+1} - T_{bn})$$



where $\tau = \Delta t$ is the time increment, Equation (7) becomes

$$T_{gn+1} = T_{gn} - \tau \left(\frac{Q_{cn} + Q_{rn}}{10.54 n_{CH_4} C_{pn}} \right) \quad (23)$$

where Q_{cn} , Q_{rn} , and C_{pn} are given by (20) and (19) and n_{CH_4} is an input representing the moles of methane in the panel volume at the time of the explosion. Equation (23) gives the gas temperature in the panel at time $t + \Delta t$ in terms of the gas temperature at time t and the total heat flow values at time t .

F.4.2.3.2 Program Section 3B

Section 3B of the program is the most complex. It solves two transient heat conduction problems assuming that the walls, floor, roof, and explosion-isolation walls are semi-infinite solids having thermal conductivities and diffusivities that may or may not be temperature dependent. In the case of the walls, floor and roof, the panel volume the conductivity and diffusivity of salt is dependent on temperature. Assuming that the explosion-isolation wall material is concrete, the conductivity and diffusivity of the explosion-isolation wall are independent of temperature.

Because of the temperature dependence of the conductivity and diffusivity of the salt, and the time-dependent spatial temperature distribution into the walls, floor and roof, the conductivity that is required for the boundary condition at $x = 0$ varies with time and the thermal diffusivity varies in both time and space. The partial differential equation for transient heat conduction when the diffusivity varies spatially is given by:

$$\frac{\partial}{\partial x} \left(\alpha \frac{\partial T}{\partial x} \right) = \frac{\partial T}{\partial t} \quad (a)$$

which can be expanded as:

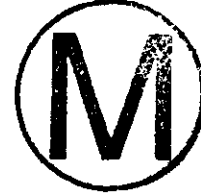
$$\left(\frac{\partial \alpha}{\partial x} \right) \left(\frac{\partial T}{\partial x} \right) + \alpha \frac{\partial^2 T}{\partial x^2} = \frac{\partial T}{\partial t} \quad (b)$$

Using the finite difference approximations,

$$\frac{\partial \alpha}{\partial x} = \frac{1}{2\epsilon}(\alpha_{m+1} - \alpha_{m-1}) \quad (\text{ci})$$

$$\alpha \frac{\partial^2 T}{\partial x^2} = \frac{\alpha_m}{\epsilon^2}(T_{m-1} - 2T_m + T_{m+1}) \quad (\text{cii})$$

$$\frac{\partial T}{\partial x} = \frac{1}{2\epsilon}(T_{m+1} - T_{m-1}) \quad (\text{cii})$$



where $\epsilon = \Delta x$, the left hand side of equation (b) becomes

$$\left(\frac{\partial T}{\partial x}\right)\left(\frac{\partial T}{\partial x}\right) + \alpha \frac{\partial^2 T}{\partial x^2} = \frac{1}{4\epsilon^2}([\alpha_{m+1} - \alpha_{m-1}][T_{m+1} - T_{m-1}] + 4\alpha_m T_{m-1} - 8\alpha_m T_m + 4\alpha_m T_{m+1}) \quad (\text{d})$$

or

$$= \frac{1}{4\epsilon^2}(\alpha_{m+1}T_{m+1} - \alpha_{m+1}T_{m-1} - \alpha_{m-1}T_{m+1} + \alpha_{m-1}T_{m-1}) + \frac{1}{4\epsilon^2}(4\alpha_m T_{m-1} - 8\alpha_m T_m + 4\alpha_m T_{m+1}) \quad (\text{e})$$

$$4\epsilon^2 \left[\left[\frac{\partial \alpha}{\partial x} \right] \left[\frac{\partial T}{\partial x} \right] + \alpha \frac{\partial^2 T}{\partial x^2} \right] = v_{m-1}(\alpha_{m-1} + 4\alpha_m - \alpha_{m+1}) - 8\alpha_m T_m + T_{m+1}(\alpha_{m+1} + 4\alpha_m - \alpha_{m-1}) \quad (\text{f})$$

Using an explicit finite difference representation of the time derivative as used in Section 3A.

$$\frac{\partial T_m}{\partial t} = \frac{1}{\Delta t}(T_{m,n+1} - T_{m,n}) \quad (\text{g})$$

Substituting (f) and (g) into the partial differential equation (a),

$$T_{m-1\ n}(\alpha_{m-1} + 4\alpha_m - \alpha_{m+1}) - 8\alpha_m T_{m\ n} + T_{m+1\ n}(\alpha_{m+1} + 4\alpha_m - \alpha_{m-1}) = \frac{1}{N}(T_{m\ n+1} - T_{m\ n}) \quad (h)$$

where

$$N = \frac{\Delta t}{4\epsilon^2} \quad (i)$$

is analogous to the modulus for the case of constant diffusion. Solving (h) for $T_{m\ n+1}$

$$T_{m-1\ n}N(\alpha_{m-1} + 4\alpha_m - \alpha_{m+1}) - (8N-1)\alpha_m T_{m\ n} + T_{m+1\ n}N(\alpha_{m+1} + 4\alpha_m - \alpha_{m-1}) = T_{m\ n+1} \quad (j)$$

For the case of constant diffusivity,

$$\alpha_{m-1} = \alpha_m = \alpha_{m+1} = \alpha$$

with

$$M = \frac{\alpha\Delta t}{\epsilon^2} = 4\alpha N \quad (k)$$



equation (j) becomes

$$T_{m\ n+1} = M(T_{m+1\ n} + T_{m-1\ n}) - (2M-1)T_{m\ n} \quad (l)$$

which is the finite difference equation for the case of constant diffusivity (Carslaw and Jaeger, 1959). Thus, equation (j) reduces to the correct equation when the diffusivity is constant and is the finite difference equation for the case of variable diffusivity.

For a numerical stability criteria,

$$M < 0.5 \quad (m)$$

the corresponding relation for the case of variable diffusivity becomes equation (n) for all m.

$$\text{MAX}(\alpha_n N) < 0.125 \quad (n)$$

The thermal conductivity and thermal diffusivity at each time point are evaluated from the temperature at that time and space as given previously for the temperature variation of the conductivity and diffusivity.

The boundary condition at $x = 0$, is the same as for the case of constant diffusivity,

$$-k_n \frac{\partial T_n}{\partial x} = q_{rn} + q_{cn} \quad (o)$$

where q_{rn} and q_{cn} are determined in Section 2. Using the finite difference relationship (Carslaw and Jaeger, 1959),

$$\frac{\partial T_n}{\partial x} = \frac{1}{2\epsilon} (-3T_{0n} + 4T_{1n} - T_{2n}) \quad (p)$$

equation (o) becomes:

$$-\frac{k_n}{2\epsilon} (-3T_{0n} + 4T_{1n} - T_{2n}) = q_{rn} + q_{cn}$$

$$3T_{0n} - 4T_{1n} + T_{2n} = \frac{2\epsilon}{k_n} (q_{rn} + q_{cn}) \quad (q)$$

Substituting for q_{rn} and q_{cn} :

$$3T_{0n} - 4T_{1n} + T_{2n} = \eta_n (T_{gn} - T_{0n}) + \gamma_n (T_{gn}^4 - T_{0n}^4)$$

where

$$\eta_n = \frac{2\epsilon h_n}{-k_n} \quad (r)$$

and

Using the identity
and defining



$$\gamma_n = \frac{2\epsilon\sigma}{k_n} \quad (s)$$

$$T_{gn}^4 - T_{0n}^4 = (T_{gn} - T_{0n})(T_{gn} + T_{0n})(T_{gn}^2 + T_{0n}^2)$$

$$f_n = (T_{gn} + T_{0n})(T_{gn}^2 + T_{0n}^2) \quad (t)$$

$$3T_{0n} - 4T_{1n} + T_{2n} = (\eta_n + \gamma_n f_n)(T_{gn} - T_{0n}) \quad (u)$$

For the case of both convection and radiation equation (u) is a fourth order equation in T_{0n} and has to be solved using a numerical technique such as Newton-Raphson iteration. Since the effect of radiation heating of the walls, floor, roof, and explosion-isolation walls leads to a more rapid cooling of the combustion gas following the explosion, and temperatures effects on the salt or explosion-isolation material is worse for longer durations, it is conservative to neglect radiation heat transfer. In this case, equation (u) becomes linear:

$$3T_{0n} - 4T_{1n} + T_{2n} = \eta_n (T_{gn} - T_{0n}) \quad (v)$$

which can be solved directly for T_{0n} :

$$T_{0n} = \frac{4T_{1n} - T_{2n} + \eta_n T_{gn}}{3 + \eta_n} \quad (w)$$

At each time the field equations are solved based on the previous time. The boundary condition (w) is then applied.

Equations (j) and (u) are formulated for both the salt comprising the walls, floor, and roof and for the explosion-isolation walls. As noted, the field equations for variable diffusivity reduce appropriately to the special case of a constant diffusivity so the above equations are sufficiently general to handle both the material of the explosion-isolation wall and the salt.

F.4.2.4 Program Section 4

In Section 4 of the program, the temperature values at time $t+\Delta t$ ($n+1$) become the new values at time t (n). The time counter, n , is incremented by 1 and the program returns to Section 1 to compute the solution at the subsequent time step.

F.4.3 Initial Volume, Surface Area and Number of Moles

The volume of gas to be cooled via heat transfer to the walls, roof, floor, and explosion-isolation walls following an explosion is taken to correspond to the effective panel volume at the time when the air-methane mixture in the panel enters the explosive range. The effective volume is defined as:

$$V_{eff} = \Phi V$$

where V is the panel volume considering closure of the panel and Φ is the porosity which accounts for the waste emplaced in the panel. Figure F-7 shows a plot of the effective volume as a function of time.

Based on Figure 4.2 of the Conceptual Design Report (DOE, 1995), the methane-air mixture in the panel volume enters the explosive range at 25 years. From Figure F-7 this corresponds to a panel volume of $1.6 \times 10^{10} \text{ cm}^3$ at the time the postulated explosion occurs.

The surface area at the time of the postulated explosion was obtained from the volume at the time the methane air mixture enters the explosive range at 25 years and the initial ratio of surface area to volume.

$$A_s = \left(\frac{A_{sinit}}{V_{init}} \right) V$$

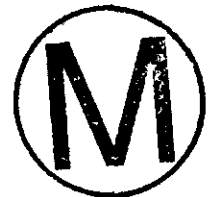


Figure F-8 shows a plot of panel surface area as a function of time.

Based on the air-methane mixture entering the explosive range at 25 years, the surface area at the time of the explosion is $1.6 \times 10^8 \text{ cm}^2$. The area of two 14 foot x 14 foot explosion-isolation walls is $1.82 \times 10^5 \text{ cm}^2$. Thus the area of the explosion-isolation walls is

$$\frac{1.82 \times 10^5}{1.6 \times 10^8} = 0.0014 = 0.14\%$$

of the total surface area.

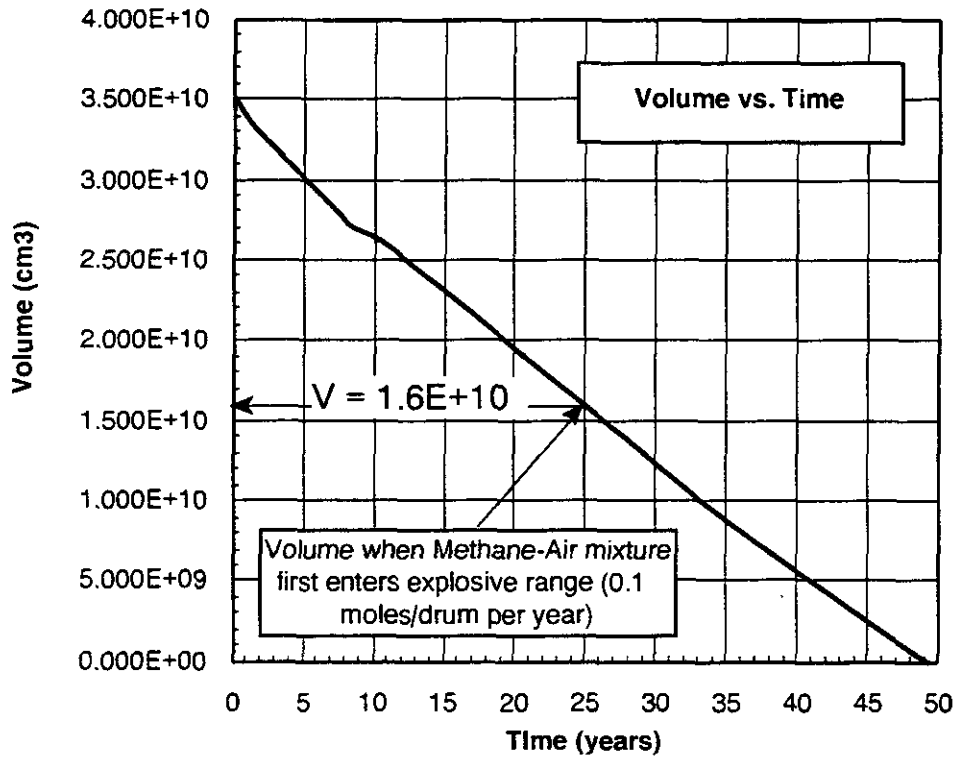


Figure F-7
Effective Panel Volume vs Time

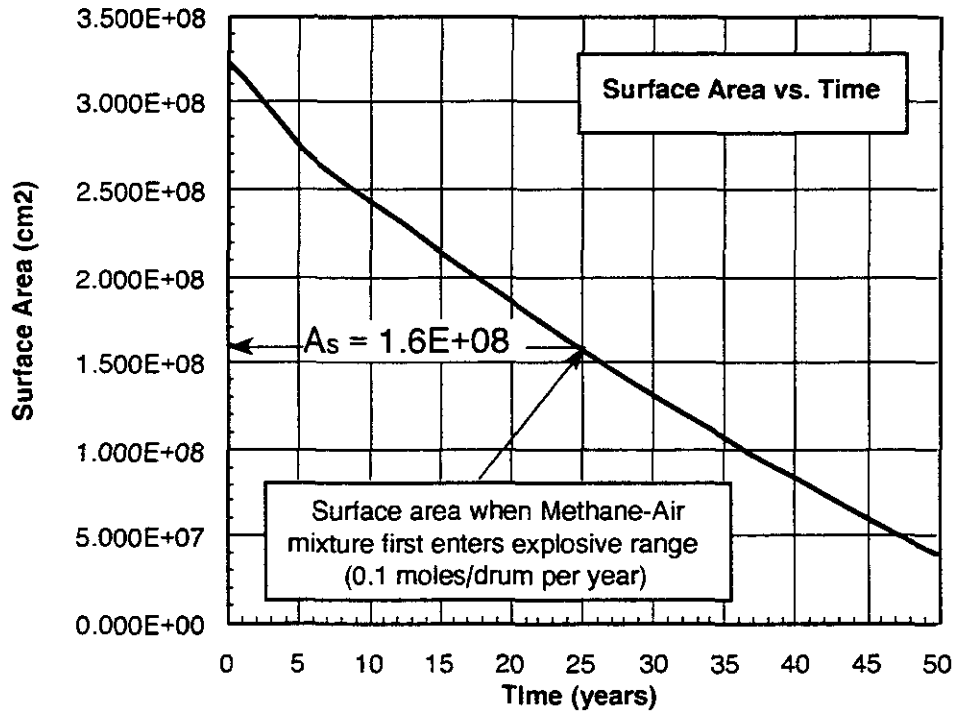
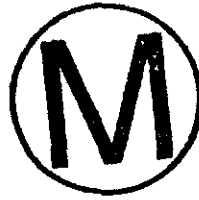


Figure F-8
Surface Area Rooms, Floor and Roof vs Time

The number of moles of combustion gas is found using the ideal gas law based on an initial pressure of 16 atmospheres (atm) and an initial temperature of 2,400 °K.

$$n = \frac{pV}{RT} \quad (24)$$

with

$$\begin{aligned} R &= 82.06 \text{ cm}^3\text{-atm/mol-}^\circ\text{K} \text{ (ideal gas law constant)} \\ p &= 16 \text{ atm} \\ V &= 1.6 \times 10^{10} \\ T &= 2400 \text{ }^\circ\text{K} \end{aligned}$$

$$n = \frac{16 \times (1.6 \times 10^{10})}{82.06 \times 2400}$$

$$n = 1.3 \times 10^6 \text{ moles}$$

The program uses the number of moles of methane and air independently to calculate the density. Thus,

$$10.54 n_{CH_4} = 1.3 \times 10^6 \quad (25)$$

$$n_{CH_4} = 1.233 \times 10^5$$

$$n_{air} = 9.54 \times n_{CH_4} = 1.176 \times 10^6$$

The density is given by

$$\frac{(1.233 \times 10^5)(16) + (1.176 \times 10^6)(29)}{1.6 \times 10^{10}} = 0.002255$$



F.5.0 Results

The numerical formulation discussed in Section 4.0 was executed using a spatial grid size, $\epsilon = 1$ cm and a time increment, $\tau = 10$ seconds. No problems with numerical stability were encountered using these values.

At time $t = 0$, the initial heat transfer from the combustion gas to the salt and explosion-isolation walls results in a large temperature gradient at the surface. To represent this gradient accurately using a finite difference formulation would require an extremely small grid spacing as the initial temperature gradient extends only an infinitesimal distance into the surface. Using a grid spacing sufficiently small to accurately characterize the initial gradient would be prohibitive, relative to the number of mesh points and time steps required.

The initial conditions for the finite difference calculations were determined by using an exact solution for the case of constant convective heat transfer coefficient and constant gas temperature. The use of the closed form solution to determine the initial conditions assumes that the change in gas temperature over small initial times is small and that the heat transfer coefficient is weakly dependent on the temperature difference between the gas and the surfaces of the salt and explosion-isolation walls. Based on the closed form solution, the initial conditions for the finite difference model were taken at a time of 12.7 seconds following the explosion. For shorter initial times, the gradient had not propagated sufficiently far into the surfaces to be represented with a 1 cm. grid spacing. Thus, the initial time for the finite difference calculations was 12.7 seconds with initial temperatures based on the closed form solution.

Figure F-9 shows the gas temperature, salt temperature (walls, floor, and roof) and explosion-isolation wall temperature as a function of time following the explosion. Figure F-10 shows the temperature distribution into the explosion-isolation walls at various times following the explosion. Figure F-11 shows the temperature distribution into the salt at various times following the explosion.

Figure F-9 shows that the temperature of the gas has nearly reached the initial ambient conditions after about 2 hours. Over that span of time, elevated temperature in the explosion-isolation wall has a maximum extent of 15 cm (about 6 inches) into the explosion-isolation wall. Since the explosion-isolation wall is at least 36 inches (91.4 cm) thick, the elevated temperature will not reach the opposite side of the wall. Thus, the assumption of a semi-infinite body in the numerical model is not violated.

A comparison of the results shown on Figure F-9 with the results given in D'Appolonia (1978) is favorable. The ratios of surface area and volume used in D'Appolonia (1978) as well as the initial pressures are not the same as used for this analysis. The temperatures shown on Figure F-9 are slightly higher than those predicted for a pressure of 9 atm as shown

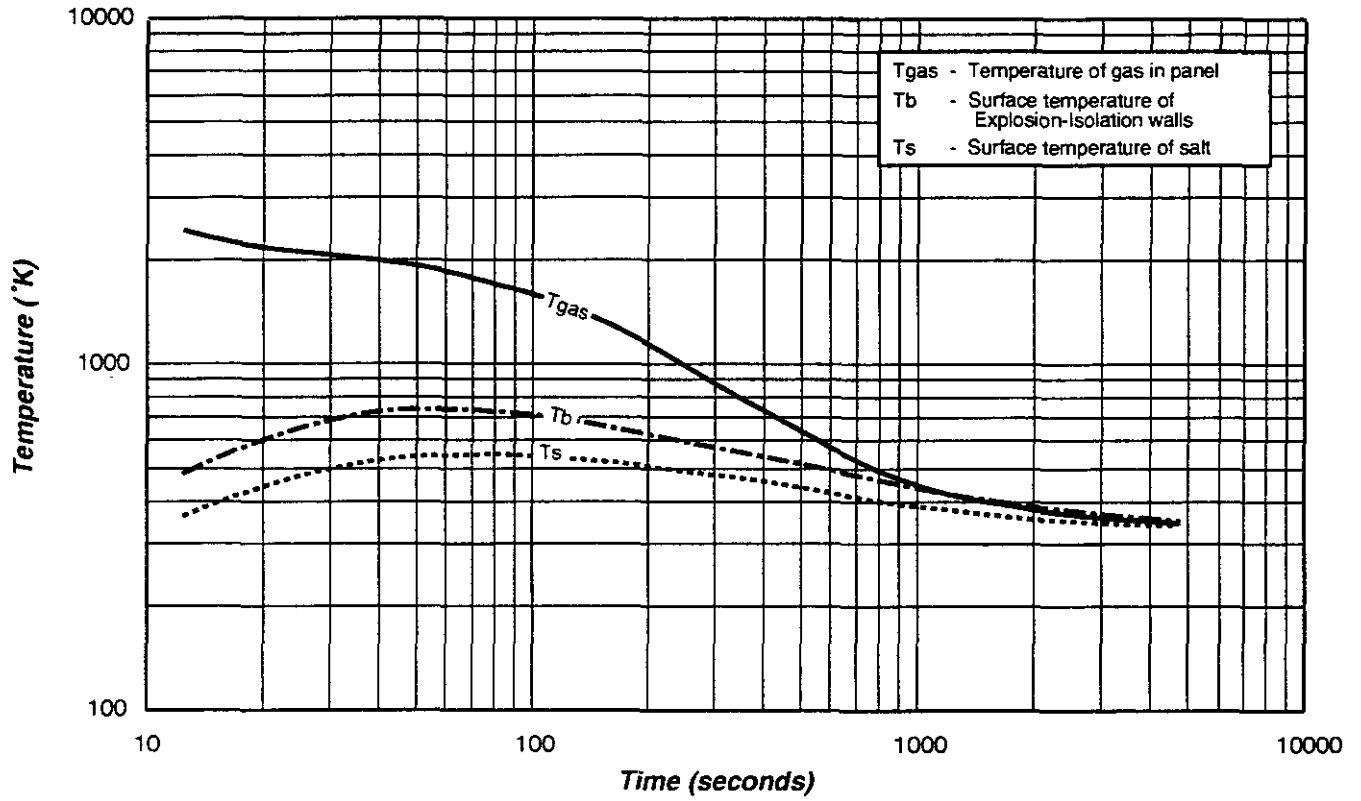


Figure F-9
Temperature Variation with Time for Gas, Salt, and Explosion-Isolation Walls

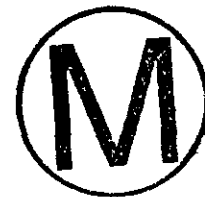
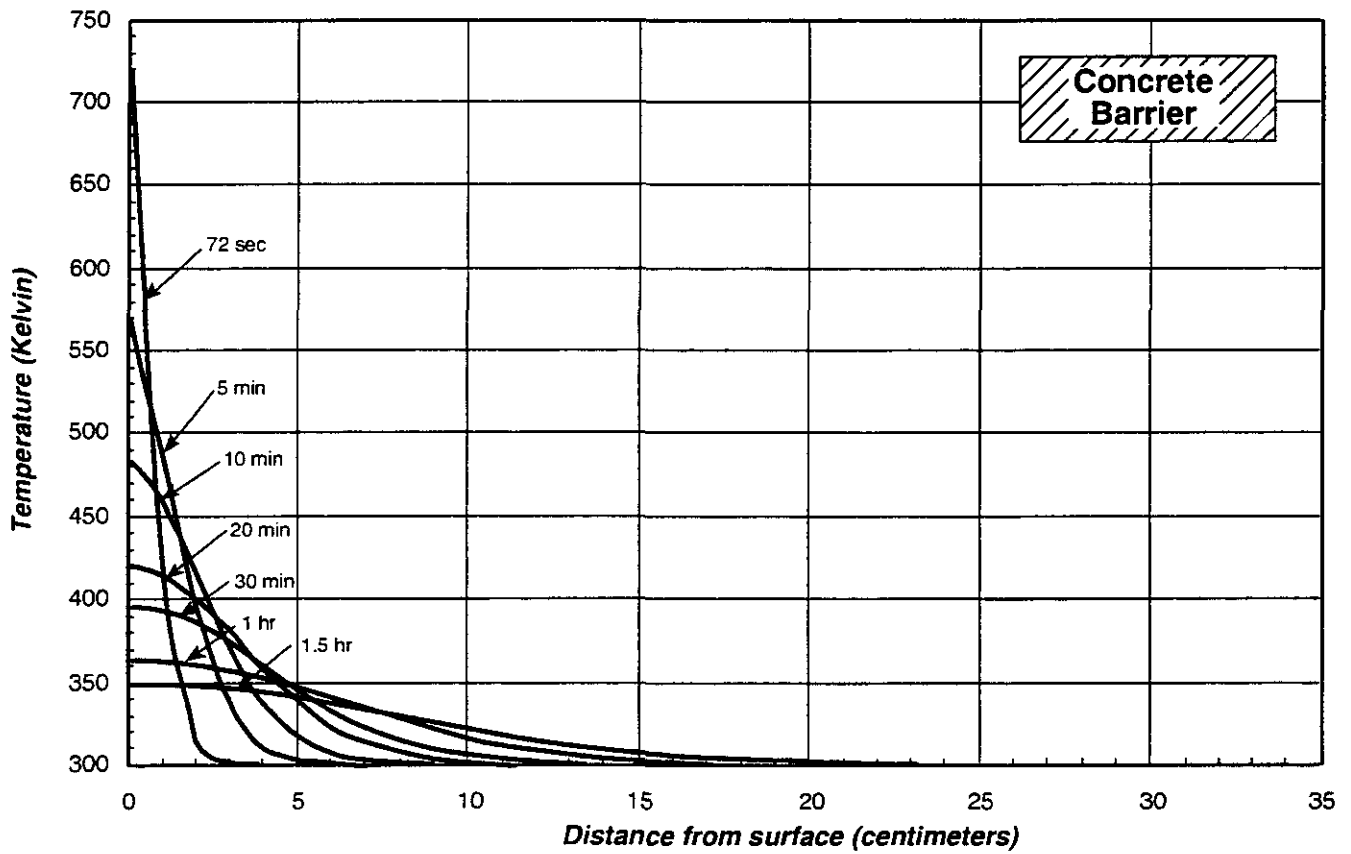


Figure F-10
Temperature Distribution with Time for Concrete Barrier

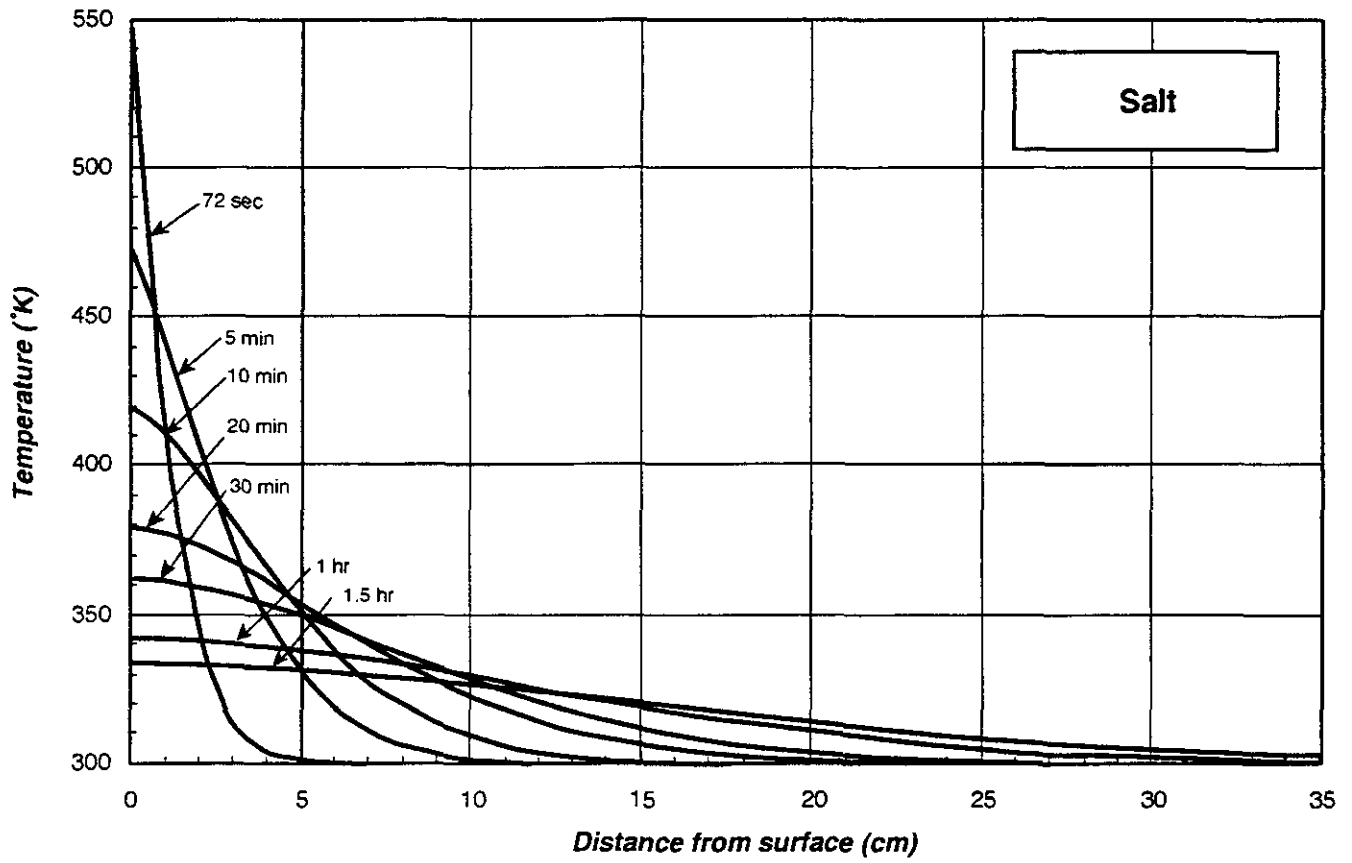


Figure F-11
Temperature Distribution with Time for Salt

in D'Appolonia [1978]. This is as expected since the initial pressure affects the number of moles which determines the rate of temperature decay in the gas. This is illustrated by comparison of the results for 9 atm with those for 27 atm shown in D'Appolonia (1978). The favorable comparison of the results shown on Figure F-9 with those of D'Appolonia (1978) provides verification of the numerical model used in these analyses.

F.6.0 References

Bodurtha, F. T., 1980, *Industrial Explosion Prevention and Control*, McGraw-Hill Book Company, New York, New York.

Carslaw, H. S., and J. C. Jaeger, 1959, *Conduction of Heat in Solids*, 2nd ed., Oxford at the Clarendon Press, Oxford, England.

D'Appolonia Consulting Engineers, 1978, "Potential for Hydrocarbon Explosions and Probable Related Impacts in Mechanically Mined Underground Crude Oil Storage Facilities," D'Appolonia Consulting Engineers, Pittsburg, Pennsylvania.

Krieg, R. D., 1983, "Reference Stratigraphy and Rock Properties for the Waste Isolation Pilot Plant (WIPP) Project," *SAND83-1908*, Sandia National Laboratories, Albuquerque, New Mexico.

Reid, R. C., J. M. Prausnitz, and T. K. Sherwood, 1977, *The Properties of Gases and Liquids*, 3rd ed., McGraw-Hill Book Company, New York, New York.

U.S. Department of Energy (DOE), 1995, "Conceptual Design for Operational Phase Panel Closure Systems," *DOE-WIPP-95-2957*, U.S. Department of Energy, WIPP Project Office, Carlsbad, New Mexico.

